SYNTHESIS AND CHARACTERIZATION OF CUBIC STRUCTURED COBALT OXIDE NANOPARTICLES CAPPED WITH TOPO THROUGH THE DECOMPOSITION OF *BIS*(N-CYCLOHEXYL-1-NAPHTHALDEHYDATO)COBALT (II) COMPLEX AS A SINGLE SOURCE PRECURSOR

T. XABA[a*], L. MOKGOERA[a], Z. NATE[a], P. M. SHUMBULA[b]
[a]*Department of Chemistry, Vaal University of Technology, P/Bag X021, Vanderbijlpark, South Africa*
[b]*Advanced Materials Division, Mintek, P/Bag X3015, Randburg, 2125, South Africa*

The synthesis of cobalt oxide nanoparticles capped with TOPO from the thermal decomposition of *bis*(N-cyclohexyl-1-naphthaldehydato)cobalt(II) complex is reported. The effect of decomposition temperature was investigated and sophisticated characterization techniques were used to characterize the complex and nanoparticles. The FTIR spectrum of the complex confirmed the formation of the precursor through the presence of the expected functional groups. The absorption and emission spectra showed an increase in wavelength when the synthetic temperature was increased. The XRD patterns of the nanoparticles displayed the formation of Co_3O_4 face-centred cubic structure. The formation of the metallic cobalt nanoparticles was also observed at higher temperature. TEM images of the cobalt oxide nanoparticles revealed spherical shaped particles.

(Received August 10, 2018; Accepted November 29, 2018)

Keywords: Cobalt complex, Tri-octylphosphine oxide, Cobalt oxide, Nanoparticles

1. Introduction

Transition metal complexes derived from Schiff bases such as 2-hydroxy-1-naphthaldehyde, salicylaldehyde etc. are one of the most malleable substances [1]. The synthesis of metal oxides nanomaterials has been an area of effective research due to many scientific applications of such materials. The study based on the synthesis and their exposures to human health is essential [2]. The performance of the nanomaterials such as their catalytic, electronic, and optical properties depends on the size and shape of the particles which is a key feature to their utmost performance and application [3-6]. Cobalt oxide in particular, is a well-recognised ferromagnetic semiconductor nanomaterial that has created a centre of attention due to its potential applications in solid-state sensors [7], magnetic materials [8], electrochemical devices [9-10], electronic and memory devices [11, 12].

Among numerous forms of cobalt oxides, Co_3O_4 and CoO are the two important types of cobalt oxides due to their distinctive structural landscapes and properties [13]. However, Co_3O_4 is the most stable phase of cobalt oxides with a direct band gap of 1.48-2.19 eV. It is also an important magnetic p-type semiconductor material [14-15]. These magnetic nanomaterials have received considerable attention recently due to their biomedical applications as drug delivery systems [16], cancer diagnosis treatment [17] etc. Several physical and chemical methods have been reported for the synthesis of cobalt oxide nanoparticles including, microwave-assisted [18], hydrothermal method [5], sol–gel techniques [19], and solution combustion method [20]. Yarestani and co-workers synthesized cobalt oxide nanoparticles through hydrothermal method and study the optical and magnetic properties of the nanomaterials [15]. Mauro *et al*. [21] reported

*Corresponding author: thokozanix@vut.ac.za

the synthesis of cobalt oxide nanoparticles. Their study was based on the behaviour of these materials towards human skin and keratinocytes toxicity.

Here, we report the preparation of *bis*(N-cyclohexyl-1-naphthaldehydato)cobalt (II) complex from the reaction of a primary amine, Schiff base ligand which is utilize in biological processes, and a cobalt salt. This complex was then used in the synthesis of Co_3O_4 nanoparticles through thermal decomposition method using TOPO as a capping molecule. The precursor was characterized with Fourier transform infrared (FTIR) spectroscopy, elemental analysis, and thermogravimetric (TGA) analysis. The synthesized cobalt oxide nanoparticles were characterized with ultraviolet–visible spectroscopy (UV-vis), photoluminescence (PL), X-ray diffraction (XRD), and transmission electron microscopy (TEM).

2. Experimental

2.1. Materials

Cobalt acetate 1142ehydrate, 2-hydroxy-1-naphthaldehyde, cyclohexamine, tri-octylphosphine oxide (TOPO), methanol, ethanol, toluene

2.2. Synthetic processes

2.2.1. Preparation of the cobalt complex [$Co(C_{17}H_{18}NO)_2$]

Bis(N-cyclohexyl-1-naphthaldehydato)cobalt (II) complex was prepared by reacting 10 mmol of 2-hydroxy-1-naphthaldehyde (HNA) in 20 mL of methanol with 10 mmol cyclohexamine in 20 mL methanol together with 5.0 mmol cobalt (II) acetate tetrahydrate in a 250 mL one necked round bottom flask. The mixture was stirred and refluxed at 50 °C for 3 hrs. The product was filtered, washed three times with ethanol and dried in an open air. The prepared complex was then weighed and characterized. The cobalt complex was obtained as a brown solid. Percentage yield: *81%. m.pt. 261 °C. CHNS analysis: Calc.: C, 72.45; H, 6.45; N, 4.97; O, 5.66%. Found: C, 73.01; H, 6.21; N, 4.99; O, 5.51%. Significant IR bands: v(C=N): 1617 cm^{-1}, v(C-O): 1533 cm^{-1}, v(C-N): 1181 cm^{-1}, v(Co-O): 510 cm^{-1} and, v(Co=N): 453 cm^{-1}.*

2.3. Synthesis of Co_3O_4 nanoparticles

TOPO-capped cobalt oxide nanoparticles were synthesized by thermal decomposition of the cobalt complex by transferring 0.5 g of the cobalt complex in 6 g TOPO using a 250 mL three-necked flask that was placed in an oil bath. The mixture was stirred and refluxed under nitrogen gas environment for 45 minutes at different temperatures of 145° and 190 °C. The solution was then cooled to 70 °C and a minimum amount of methanol was added into the flask. The product was centrifuged, washed three times with methanol and dried. The resulting TOPO-capped cobalt oxide nanoparticles were dispersed in toluene for further characterization.

2.4. Characterization of the precursor and cobalt oxide nanoparticles

Microanalysis was collected on a Perkin-Elmer automated model 2400 series II CHNS/O elemental analyser. Fourier transform infrared (FTIR) spectroscopy analysis of the cobalt complex was operated at room temperature in a scan range between 4000 to 400 cm^{-1} from a Bruker FTIR tensor 27 spectro-photometer. A Perkin-Elmer Pyris 6 TGA was ran at 20 °C/min at a heating rate from 30-900 °C in a closed punctured aluminium pan under nitrogen gas environment was used to accomplish the thermal analysis. The absorption and emission spectra of cobalt oxide nanoparticles were achieved through UV-1800 Shimadzu spectrophotometer and Gilden Fluorescence. The XRD patterns were collected through the Phillips X'Pert diffractometer with secondary monochromated Cu Kα radiation (λ = 1.54060 A°) at 40 kV/30mA at 2θ = 10-90° and the TEM images were assembled at an accelerating voltage of 300 kV from a Tecnai F30 FEG TEM instrument.

3. Results and discussions

The synthesis of cobalt oxide nanoparticles using thermal decomposition of *bis*(N-cyclohexyl-1-naphthaldehydato)cobalt (II) complex at various temperatures using TOPO as a capping agent is reported. The cobalt complex was obtained as shown in Scheme 1 below:

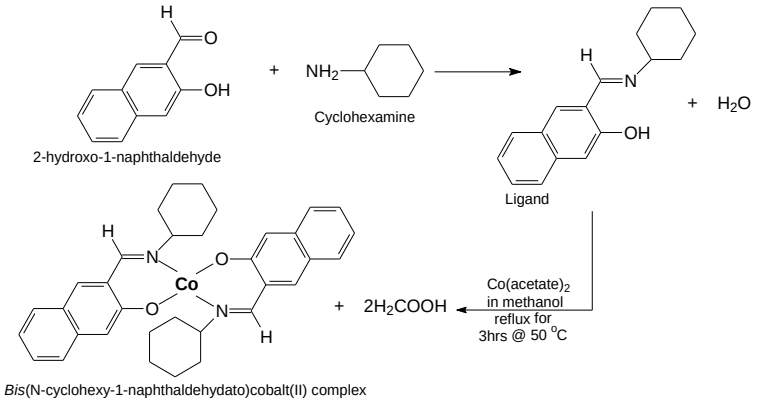

Scheme 1. The preparation of the bis(N-cyclohexyl-1-naphthaldehydato)cobalt (II) complex.

3.1. Spectroscopic and Thermal studies of the Cobalt complex

Fig. 1(a) shows the FTIR spectrum of *bis*(N-cyclohexyl-2-hydroxy-1-naphthaldehydato)cobalt (II) complex which displayed the broad absorption bands between 3305-3046 cm^{-1} that correspond to O–H stretching vibrations from the solvent that was used for washing and the characteristic –C–H peaks from the benzene ring were sported at 2926-2353 cm^{-1}. The strong bands were observed at 1618–1536 cm^{-1} which are attributed to the stretching vibrations of C=N groups. The phenolic C–O stretching vibration was observed at 1388 cm^{-1} and the strong band at 1181 cm^{-1} which was ascribed to C–N stretching vibration. The stretching bands that verify the coordination of nitrogen and oxygen to the cobalt ion were also observed at 517 and 462 cm^{-1} which correspond to Co–O and Co–N bonds. Similar observation was reported by Sebastian and co-workers [22].

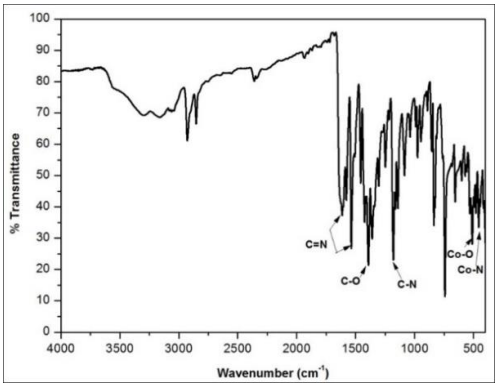

Fig. 1. FTIR spectrum (a) and TGA/DTG curves of bis(N-cyclohexyl-1-naphthaldehydato)cobalt (II) complex

Thermogravimetric analysis (TGA) coupled with differential thermogravimetric analysis (DTG) were used to investigate the decomposition temperature of the precursors under nitrogen atmosphere at the temperature ranging from 20 to 900 °C. TGA graph of the cobalt complex in Fig. 2 shows four decomposition stages. The first decomposition peak at 179-209 °C with a partial

weight loss of 3% can be ascribed to the loss of the nitrates [23]. The second and the third decomposition between 339-356 and 373-471 °C with the total weight loss of 62% is attributed to the elimination of some of the precursor constituents leaving cobalt oxide. The last decomposition between 582-625 °C is due to the reduction of Co_3O_4 to CoO [24-25] which was also confirmed by the DTG results.

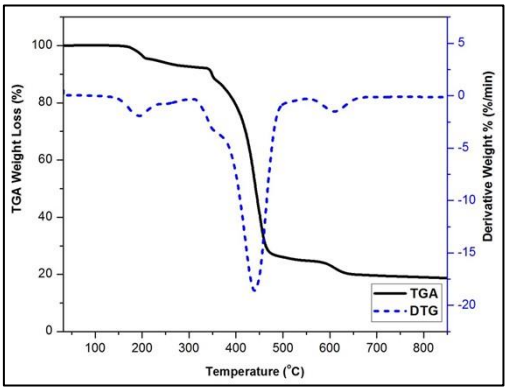

Fig. 2. TGA and DTG curves of bis(N-cyclohexyl-1-naphthaldehydato)cobalt (II) complex.

3.2. Optical properties

Fig. 3 shows the UV-vis absorption spectra of the synthesized cobalt oxide nanoparticles synthesized at 145 and 190 °C. The optical absorption spectra exhibited well-defined peaks at 391 and 396 nm which was increasing as the temperature was increased. Their band gap energies were calculated according to following equation [26]:

$$\alpha h\nu = K(h\nu - E_g)^n \quad (1)$$

where α is the absorption coefficient, h is the Planck constant, ν is the light frequency, K is a constant, Eg is the band gap, and n = 2 for the direct band gap and n = 1/2 for the indirect band gap. Extrapolation of the linear section can contribute Eg values. The band gaps of as-synthesized Co_3O_4 nanoparticles were found to be 3.07 and 2.73 eV which is larger than the previously reported value for the Co_3O_4 bulk material [14].

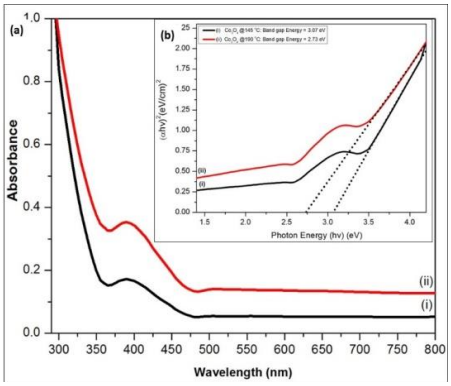

Fig. 3. Absorption spectra (a) and Tauc plot (b) of the cobalt oxide nanoparticles capped with TOPO synthesized at 145 (i) and 190 °C (ii).

The luminescence properties of the cobalt oxide nanoparticles were investigated at room temperature on excitation wavelength of 400 nm. The emission spectra of Co_3O_4 nanoparticles

synthesized at the temperatures of 145 and 190 °C in Fig. 4 demonstrate the strong broad emission minima at 431 and 435 nm in the visible region that were red-shifted from their absorption edges. The strong emission peaks signify the high crystalline character of the synthesized Co_3O_4 nanoparticles [27].

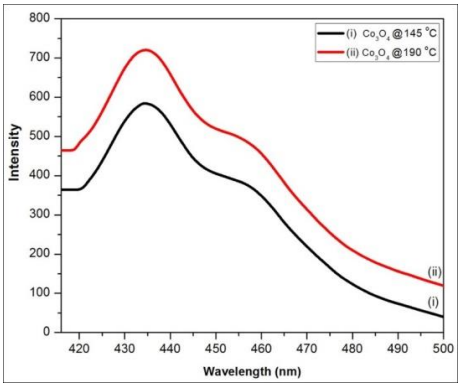

Fig. 4. Emission spectra of the cobalt oxide nanoparticles capped with TOPO synthesized at 145 (i) and 190 °C (ii).

3.3. Structural properties

The X-ray diffraction patterns of TOPO capped Co_3O_4 nanoparticles synthesized at different temperatures of 145 and 190˚C is represented in Fig. 5. The prominent peaks at 19.62, 31.40, 36.03, 45.85, 54.59, 59.74, and 64.92˚ that correspond to (111), (220), (311), (222), (400), (511), and (440) planes can be indexed to Co_3O_4 face-centred cubic structure [JCPD: 42-1467] with lattice parameter of a=b=c=6.85 Å. The pattern of the TOPO capped Co_3O_4 nanoparticles synthesized at higher temperature displayed another set of peaks at 44.07, 50.12, and 77.59˚correspond to (111), (200), and (220) planes that can be indexed to metallic Co cubic structure [JCPD: 15-0806]. The extra XRD peak which appears in both patterns that is located around 24.80˚ can be ascribed to the capping molecule.

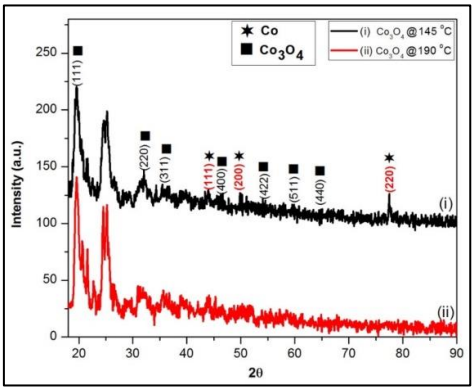

Fig. 5. X-ray diffraction patterns of the cobalt oxide nanoparticles capped with TOPO synthesized at 145 (i) and 190 °C (ii).

The size of nanomaterial plays a crucial role in manipulating the properties of particles. The TEM analysis was conducted to confirm the morphology of cobalt oxide nanoparticles. The images of the nanomaterials synthesized at 145 and 190 °C are represented in Fig. 6. The nanoparticles that were prepared at lower temperature (Fig. 6(a)) displayed the mixture of sheet-like structures and spherical particles with an average particle sizes of 5.23±0.957 nm which is represented by the frequency distribution bar graph in Fig. 6(b). The well-distributed

spherical particles in Fig. 6(c) with the average particle sizes of 7.28±0.737 nm that is confirmed by the frequency distribution graph in Fig. 6(d) were observed.

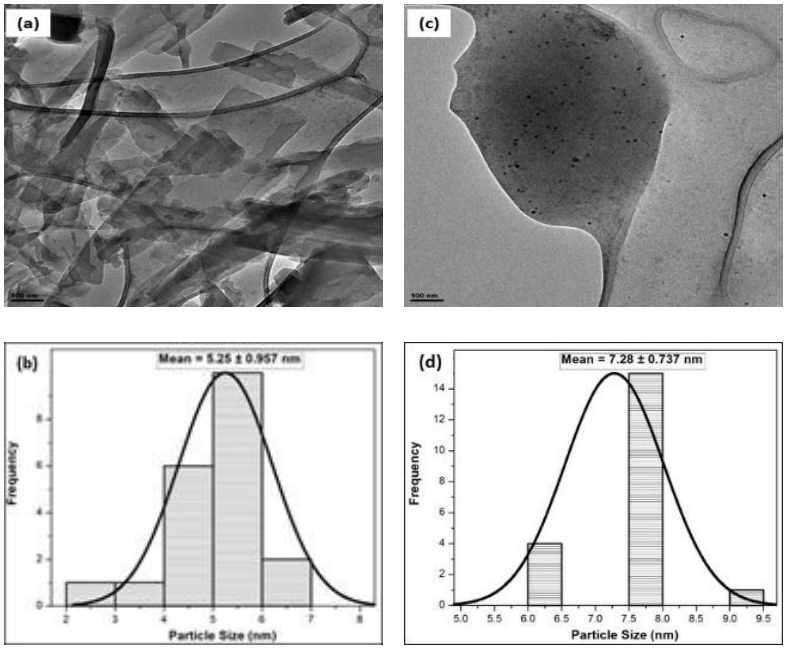

Fig. 6. TEM images and frequency distribution of the cobalt oxide nanoparticles capped with TOPO synthesized at 145 (a) & (b) and 190 °C (c) & (d).

4. Conclusions

Bis(N-cyclohexyl-1-naphthaldehydato)cobalt (II) complexes have been prepared through simple one step method and used as a precursor to synthesize cobalt oxide nanoparticles. The absorption and emission peaks were red shifted toward the higher wavelength while their band gap energies were decreasing when the temperature was increased. The XRD patterns of the cobalt oxide nanoparticles exhibited face-centred cubic structure nanomaterials. The mixture of Co_3O_4 and metallic Co nanoparticles was observed on the nanoparticles that were prepared at higher temperature. The TEM images of the nanomaterials presented well-shaped and monodispersed particles at higher temperature.

Acknowledgements

Authors would like to thank the National Research Foundation (NRF) (Thuthuka Grant Holder no: TTK170508230117) and the Vaal University of Technology for funding this project.

References

[1] C. Biswas, M. G. B. Drew, A. Figuerola, S. Gómez-Coca, E. Ruiz, V. Tangoulis, A. Ghosh, Inorg. Chim. Acta. **363**(5), 846 (2010).
[2] G. Oberdörster, E. Oberdörster, J. Oberdörster, Environ Health Perspect. **113**(7), 823 (2005).
[3] Y. Dong, K. He, L. Yin, A. Zhang, Nanotechnology. **18**(43), 435602 (2007).
[4] L. M. Alrehaily, J. M. Joseph, M. C. Biesinger, D. A. Guzonas, J. C. Wren, Phys. Chem. Chem. Phys. **15**(3), 1014 (2013).
[5] M. M. Rahman, J. Z. Wang, X. L. Deng, Y. Li and H. -K. Liu, Electrochim. Acta. **55**(2), 504 (2009).

[6] Y. Zhang, Y. Chen, T. Wang, J. Zhou, Y. Zhao, Microporous Mesoporous Mater. **114**(1-3), 257008).
[7] W. Y. Li, L. N. Xu, J. Chan, Adv. Funct. Mater. **15**(5), 851 (2005).
[8] C. Nethravathi, S. Sen, N. Ravishankar, M. Rajamathi, C. Pietzonka, B. Harbrecht, J. Phys. Chem. B. **109**(23), 11468 (2005).
[9] X. Wang, X. Y. Chen, L. S. Gao, H. G. Zheng, Z. Zhang, Y. T. Qian, J. Phys. Chem. B. **108**(42), 16401 (2004).
[10] C. S. Cheng, M. Serizawa, H. Sakata, T. Hirayama, Mater. Chem. Phys. **53**(3), 225 (1998).
[11] S. A. Wolf, D. D. Awschalom, R. A. Buhrman, J. M. Daughton, S. von Molnár, M. L. Roukes, A. Y. Chtchelkanova, D. M. Treger, Science. **294**(5546), 1488 (2001).
[12] B. K. Pandey, A. K. Shahi, Ram Gopal, Applied Surface Science. **347**, 461 (2015).
[13] R. Shi, G. Chen, W. Ma, D. Zhang, G. Qiu, X. Liu, Dalton Trans. **41**(19), 5981 (2012).
[14] Y. Teng, S. Yamamoto, Y. Kusano, M. Azuma, Y. Shimakawa, Mater. Lett. **64**(3), 239242 (2010).
[15] M. Yarestani, A. D. Khalaji, A. Rohani, D. Das, Islamic Republic of Iran. **25**(4), 339 (2014).
[16] E. P. Da Silva, D. L. Sitta, V. H. Fragal, T. S. Cellet, M. R. Mauricio, F. P. Garcia, C. V. Nakamura, M. R. Guilherme, A. F. Rubira, M. H. Kunita, Int. J. Biol. Macromol. **67**, 43 (2014).
[17] H. C. Chen, J. T. Qiu, F.L. Yang, Y. C. Liu, M. C. Chen, R. Y. Tsai, H. W. Yang, C. Y. Lin, C. C. Lin, T. S. Wu, Y. M. Tu, M. C. Xiao, C. H. Ho, C. C. Huang, C. S. Lai, M. Y. Hua, Anal. Chem. **86**(19), 9443 (2014).
[18] S. Vijayakumar, A. K. Ponnalagi, S. Nagamuthu, G. Muralidharan, Electrochim. Acta. **106**, 500013).
[19] A. U. Mane, K. Shalini, A. Wohlfart, A. Devi, S. A. Shivashankar, J. Cryst. Growth. **240**(1-2), 157 (2002).
[20] J. C. Toniolo, A. S. Takimi, C. P. Bergmann, Materials Research Bulletin. **45**(6), 672 (2010).
[21] M. Mauro, M. Crosera, M. Pelin, C. Florio, F. Bellomo, G. Adami, P. Apostoli, G. De Palma, M. Bovenzi, M. Campanini, F. L. Filon, Int. J. Environ. Res. Public Health. **12**(7), 8263 (2015).
[22] M. Sebastian, V. Arun, P. P. Robinson, A. A. Varghese, R. Abraham, E. Suresh, K. K. M. Yusuff, Polyhedron. **29**(15), 3014 (2010).
[23] T. Xaba, B. W. Masinga, M. J. Moloto, Digest Journal of Nanomaterials and Biostructures **11**(4), 1231 (2016).
[24] B. M. Abu-Zied, S.A. Soliman, Catal. Lett. **132**(3-4), 299 (2009).
[25] M. T. Makhlouf, B. M. Abu-Zied, T. H. Mansoure, Physical Chemistry. **2**(6), 86 (2012).
[26] J. Zhang, Z. Liu, Z. Liu, ACS Applied Materials & Interfaces. **8**(15), 9684 (2016).
[27] T. Xaba, M. J. Moloto, O. Nchoe, Z. Nate, N. Moloto, Chalcogenide Letters. **14**(8), 337 (2017).